

## Excitonic Absorption in a Quantum Dot

P. Hawrylak and G. A. Narvaez\*

*Institute for Microstructural Science, National Research Council of Canada, Ottawa, Ontario, Canada K1A 0R6*

M. Bayer and A. Forchel

*Technische Physik, Universität Würzburg, Am Hubland, D-97094 Würzburg, Germany*

(Received 10 December 1999)

The excitonic absorption spectrum of a single quantum dot is investigated theoretically and experimentally. The spectrum is determined by an interacting electron–valence-hole complex. We show that the mixing of quantum configurations by two-body interactions leads to distinct absorption spectra controlled by the number of confined electronic shells. The theoretical results are compared with results of photoluminescence excitation spectroscopy on a series of single self-assembled  $\text{In}_{0.60}\text{Ga}_{0.40}\text{As}$  quantum dots.

PACS numbers: 71.35.Cc, 73.20.Dx, 78.55.Cr, 85.30.Vw

In this Letter we determine the ground and excited states of an exciton in zero-dimensional systems [1,2]. The variation of the exciton density of states of a single self-assembled quantum dot [3,4] with size is measured by photoluminescence excitation (PLE) spectroscopy [5,6]. We find features in the absorption spectra which were not observed in spectra from large ensembles of dots [7]. These features can be understood by constructing a theoretical model of an exciton in a “coherent exciton” basis. The basis captures important symmetries of the interacting electron-hole pair. The trivial variation of the single particle shell structure is translated into a nontrivial modification of the interacting electron hole system.

The lens-shaped self-assembled quantum dots (SAD) are excellent models of zero-dimensional (0D) systems. In these structures the single particle states  $|n, m\rangle$  can be well approximated by those of a pair of harmonic oscillators with quantum numbers  $m$  and  $n$  [8]. These states form a finite number of degenerate shells  $S = m + n$  with degeneracies  $g_S = S + 1$  and energies  $E(S) = \Omega S$ , where  $\Omega = \Omega_{e(h)}$  for electrons and holes. The angular momentum of electrons is  $l^e = n_e - m_e$ . The angular momentum of holes is opposite to the electrons. The electrons and holes interact with each other via Coulomb interaction. The exciton Hamiltonian can be written in any basis of electron-hole states [8]. We focus here on the construction of a basis which captures all the symmetries of the problem and allows us not only to compute but also to understand the exciton spectrum and its dependence on the number of electronic shells. The exciton states are a superposition of a product of electron and hole states  $|i\rangle|j\rangle$  (where  $|i\rangle = |n_e, m_e\rangle$ ). Coulomb scattering conserves the total angular momentum  $R = l_i - l_j$  of a pair and all states can be classified by their total angular momentum. The absorption spectrum  $A(\omega)$  of a photon with frequency  $\omega$  due to transitions from the initial vacuum state  $|0\rangle$  of a SAD to all final states  $|i\rangle$  is given by Fermi’s golden rule:  $A(\omega) = \sum_i |\langle i|\mathcal{P}^\dagger|0\rangle|^2 \delta(\omega - (\mathcal{E}_i - \mathcal{E}_0))$ . Here  $\mathcal{E}_i$  and  $\mathcal{E}_0$  are the energies of the final and initial

states of the absorption process. Initial and final states are coupled through the interband polarization operator  $\mathcal{P}^\dagger|0\rangle = \sum_j |j\rangle|j\rangle$ .  $\mathcal{P}^\dagger$  creates electron-hole pairs in identical orbitals  $j$ , i.e., with zero total angular momentum of the pair. Let us rename orbitals in terms of their shell index  $S$  and angular momentum  $l$  as  $|S, l\rangle$ . We can now generate and classify electron-hole pairs with zero total angular momentum. These states fall into two classes. In each shell  $S$ , there are what appear to be optically active pairs of the form  $|S, l\rangle|S, -l\rangle$ . Their number equals the degeneracy of each shell  $S + 1$  and the energy of each pair is  $(\Omega_e + \Omega_h)S = \iota S$ . Pairs in different shells have different energy. The density of states corresponding to these pairs in a dot with three shells is shown in Fig. 1a. While these pairs correspond to vertical transitions, photons do not create individual pairs but rather a linear superposition of them  $\mathcal{P}^\dagger|0\rangle = \sum_S [\sum_l |S, l\rangle|S, -l\rangle]$ . Hence only one “coherent” state  $|S\rangle = \sum_l |S, l\rangle|S, -l\rangle$  from each  $S + 1$  degenerate shell couples to photons. The remaining  $S$  states are dark. It is therefore convenient to create a coherent exciton representation which explicitly accounts for this symmetry. This is done by a transformation into Jacobi-like coordinates where one of the orthogonal basis states is the coherent state  $|S\rangle$ . In Jacobi coordinates one can immediately decide which states are coupled to the coherent state by Coulomb interactions and become optically active. In fact, for symmetric interactions  $V_{ee} = V_{hh} = -V_{eh}$  coherent states are exact eigenstates of the interacting exciton Hamiltonian restricted to a given shell. Hence even in the presence of interactions each shell contains exactly one optically active configuration. This symmetry and procedure is analogous to Kohn’s theorem for intraband transitions and can be loosely described as “Kohn’s theorem for excitons” [9].

The next step is the search for other possible two-particle configurations. The most important configurations, if they exist, are those with energy resonant with coherent exciton states. At first glance the only candidates are pairs of states from different shells, e.g.,  $|S, l\rangle|S', -l\rangle$ . The energy

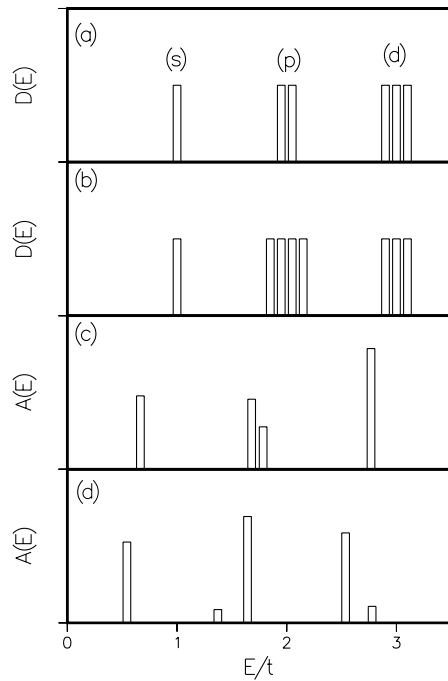


FIG. 1. (a) Density of states of optical transitions; (b) density of states of an exciton in coherent exciton representation showing degeneracies of excitonic shells; (c),(d) calculated absorption spectra showing the splitting of the  $p$ -like transition for different sets of quantum dot parameters.

of these states  $\Omega_e S + \Omega_h S'$  is different from the energy of coherent exciton states. It is therefore difficult to expect these states to acquire a significant oscillator strength apart from accidental, parameter dependent, degeneracies. However, when we construct a superposition of these electron-hole states from different shells in the form

$$|S, p\rangle = \frac{1}{\sqrt{2}} (|S - p, l\rangle |S + p, -l\rangle \pm |S + p, l\rangle |S - p, -l\rangle), \quad (1)$$

we find that their energy,

$$E(S, p) = \frac{1}{2} [\Omega_e(S - p) + \Omega_h(S + p)] + [\Omega_e(S + p) + \Omega_h(S - p)], \quad (2)$$

equals the energy  $(\Omega_e + \Omega_h)S$  of the coherent exciton state in shell  $S$ . What is even more important, this conclusion is valid for any ratio of the electron and hole kinetic energy. These configurations have not been constructed from Jacobi coordinates and therefore Coulomb interactions mix them with coherent exciton states. The mixing makes configurations with a  $+$  sign optically active. These are precisely the nontrivial states which strongly modify the absorption spectrum. We can immediately construct degenerate shells of electron-hole states with degeneracies depending on the number of confined single particle levels  $(n, m)$ . For two shells  $(s, p)$  we have degeneracies  $(1, 2)$ , for three shells  $(s, p, d)$  we have  $(1, 4, 3)$ ,

while for five shells we have  $(1, 4, 9, 12, 5)$ . Hence degeneracies of excitonic shells depend on the number of confined single particle levels. It is best to illustrate these constructions on a simple example of a dot with two and three shells.

For a dot with three lowest shells  $S = 0, 1, 2$ , there are six optically active configurations ( $a-f$ ):  $(|00\rangle|00\rangle)$ ,  $(|11\rangle|1-1\rangle, |1-1\rangle|11\rangle)$ ,  $(|22\rangle|2-2\rangle, |2-2\rangle|22\rangle, |20\rangle|20\rangle)$ . In addition there are two configurations ( $g, h$ ) originating from different shells:  $(|00\rangle|20\rangle)$ ,  $(|20\rangle|00\rangle)$ . These optically inactive states involve a hole (electron) in the zero angular momentum state  $|00\rangle$  of the  $s$  shell and a hole (electron) in the zero angular momentum state  $|20\rangle$  of the  $d$  shell. They are degenerate with coherent exciton states of a  $p$  shell. Hence an exciton is composed of eight states with zero total angular momentum. The next step is the transformation into coherent exciton states (Jacobi coordinates). The  $s$  shell is unchanged,  $|A\rangle = |a\rangle$ . The  $p$  shell contains two configurations:  $|B\rangle = \frac{1}{\sqrt{2}}(|b\rangle + |c\rangle)$  and  $|C\rangle = \frac{1}{\sqrt{2}}(|b\rangle - |c\rangle)$ . The  $d$  shell is replaced with  $|D\rangle = \frac{1}{\sqrt{3}}(|d\rangle + |e\rangle + |f\rangle)$ ,  $|E\rangle = \frac{1}{\sqrt{2}}(|d\rangle - |e\rangle)$ , and  $|F\rangle = \frac{1}{\sqrt{6}}(|d\rangle + |e\rangle - 2|f\rangle)$ . The two configurations ( $g, h$ ) are replaced with  $|H\rangle = \frac{1}{\sqrt{2}}(|g\rangle + |h\rangle)$  and  $|G\rangle = \frac{1}{\sqrt{2}}(|g\rangle - |h\rangle)$ . The density of states of an electron-hole pair in Jacobi coordinates is shown in Fig. 1b. The key result is that there are now four degenerate states  $B, C, G, H$  in the  $p$  shell. The Jacobi coordinates allow us to separate the optically active states from the dark states in the interacting system. By expanding the interband polarization operator in the new basis  $\mathcal{P}^\dagger|0\rangle = |A\rangle + \sqrt{2}|B\rangle + \sqrt{3}|D\rangle$  we see that only three coherent states,  $|A\rangle$ ,  $|B\rangle$ , and  $|D\rangle$ , are optically active. Clearly states  $|C\rangle$ ,  $|E\rangle$ ,  $|G\rangle$ , which are the antisymmetric superpositions of pair states, cannot couple to remaining states. Therefore, there are five active states: state  $|A\rangle$  from the  $s$  shell, states  $|B\rangle$  and  $|H\rangle$  from the  $p$  shell, and states  $|D\rangle$  and  $|F\rangle$  from the  $d$  shell. Hence the spectrum of SAD with three shells will consist of five peaks: one derived from the  $s$  shell, two from the  $p$  shell, and two from the  $d$  shell. The calculated absorption spectra  $A(\omega)$  showing the splitting of the  $p$ -shell transition are shown in Figs. 1c and 1d. In Fig. 1c the  $\Omega_e = \Omega_h$  and masses are the same. In Fig. 1d the  $\Omega_e = 2\Omega_h$  and the mass of the hole is twice the mass of the electron. In addition, a small splitting of the  $d$ -shell energy levels was introduced to simulate the energy levels of lens-shaped self-assembled quantum dots. In the absence of interactions the transition energies (Fig. 1a) are equally spaced in units of electron-hole energy  $t$ . The inclusion of the  $e-h$  scattering changes the absorption spectrum. The attractive electron-hole interaction renormalizes transition energies and leads to additional structures in the spectrum. The most important effect is the splitting of the  $p$ -shell absorption in Figs. 1c and 1d. The oscillator strength depends on parameters: it is almost equally distributed between the  $p$ - $p$ -like

transition  $|B\rangle$  and the  $s$ - $d$ -like transition  $|H\rangle$  in Fig. 1c but changes oscillator strength in Fig. 1d. The absorption into the  $d$  shell is also split into two lines, one strong and one weak, and the oscillator strength depends on dot parameters. It is important that the splitting of the  $p$ -shell absorption is an excitonic feature due to mixing of configurations. These configurations, and the splitting, become possible in dots with at least three electronic shells and are absent in dots with only two shells. The splitting is not related to the splitting of single particle levels due to dot asymmetries. To test these predictions experimentally we chose identical  $\text{In}_{0.60}\text{Ga}_{0.40}\text{As}$  self-assembled quantum dots with different sizes: one dot with only two shells and one dot with three shells.

The single  $\text{In}_{0.60}\text{Ga}_{0.40}\text{As}$  SAD have been studied by photoluminescence (PL) and PLE spectroscopy. Figure 2 shows PL spectra of mesa structures of the two samples containing millions of dots [10]. At low optical excitation emission from the ground  $s$  shell and from the wetting layer can be seen in both types of dots. With increasing excitation power, emission from higher confined shells is observed. For the first type of dots (upper panel) only two shells are confined: besides emission from the twofold degenerate  $s$ -shell emission from the first excited  $p$  shell is detected, which is fourfold degenerate (including the spin degrees of freedom). In contrast, for the second type of dots (lower panel) one more shell, the sixfold-degenerate  $d$  shell becomes confined. Thus these two samples allow

us to study the modification of the exciton states, when the number of single particle orbitals is doubled.

Spectroscopic resolution of single dots was obtained by a lithographic patterning of the as-grown samples, as described earlier. To test the theoretical predictions, quantum dots exhibiting degenerate single particle shells are required. Degeneracies could be lifted by dot shape asymmetries leading also to a splitting of the  $p$  shell [11]. The quantity which is very sensitive to asymmetries is the exciton fine structure due to the electron-hole exchange interaction. Shape asymmetries lead to a linear polarization splitting of the exciton emission. For the present studies we have selected only dots for which no such splitting is observed. This is a clear indication for a rotational symmetry of the structures around the heterostructure growth direction leading to angular momentum degeneracy.

Figure 3 shows characteristic PL (dotted traces) and PLE (solid traces) spectra of a pair of single quantum dots of type 1 (upper panel) and one of type 2 (lower panel). In the low excitation PL spectra a single sharp emission line with a half-width of about 0.1 meV is observed. For the PLE studies the detection wavelength was set to this  $s$ -shell recombination energy. The case of a type-1 dot can be easily derived from the above considerations: only the first three states of Fig. 1a need to be considered. Their transformation to Jacobi coordinates gives the states  $|A\rangle$ ,  $|B\rangle$ , and  $|C\rangle$ . The last state is optically inactive. Therefore only two absorption lines are observed in the absorption

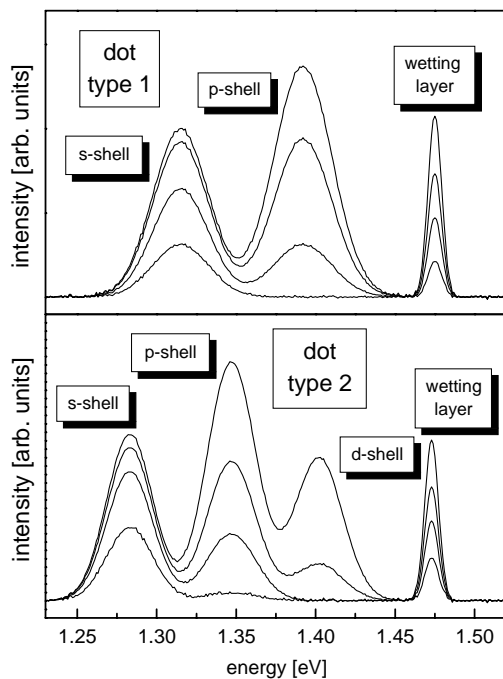


FIG. 2. Photoluminescence spectra on arrays of  $\text{In}_{0.60}\text{Ga}_{0.40}\text{As}$  self-assembled dots recorded for varying excitation power by an  $\text{Ar}^+$  laser at  $T = 2$  K. In the type-1 dots sample (upper panel) only two electronic shells are confined in the dots; in the type-2 dot sample (lower panel) three shells are confined.

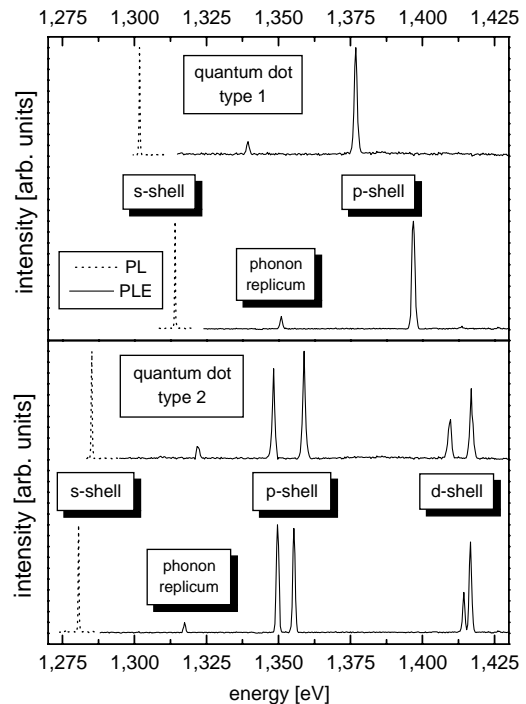


FIG. 3. Photoluminescence excitation spectra ( $T = 2$  K) of single  $\text{In}_{0.60}\text{Ga}_{0.40}\text{As}$  self-assembled dots of type 1 (upper panel) and of type 2 (lower panel). Excitation source was a tunable Ti-sapphire laser.

spectra as displayed in Fig. 3. For the dots of type 1 only a single sharp absorption line of strong intensity is observed between the  $s$ -shell exciton energy and the energy of the wetting layer recombination. Its energy corresponds well with the energy of the  $p$ -shell emission in Fig. 2. Note also that a phonon replicum is observed, which is located 36.7 meV above the  $s$ -shell exciton. However, its intensity is more than an order of magnitude weaker than the  $p$ -shell exciton absorption. This is an indication that the system exhibits in good approximation charge neutrality; that is to say, an exciton in the quantum dot does not have a large dipole momentum nor does the dot contain additional charges. Otherwise the phonon replica intensity would be expected to be much stronger.

The phonon replicas are also very weak for dots of type 2. However, now a doublet of strong absorption lines of comparable oscillator strength is observed for the  $p$  shell. The energy splitting between the two spectral lines is about 8.5 meV for the lower and 10.5 meV for the upper spectrum. We identify the two lines as originating from configurations  $|B\rangle$  and  $|H\rangle$ . The calculated energy splittings are 10 meV for Fig. 1c with  $t = 100$  meV and 19 meV for Fig. 1d with  $t = 70$ . The actual values do of course depend on the parameters of the dot and a choice of different effective masses can achieve a superficial quantitative agreement with the experiment. In the  $d$  shell a doublet of emission lines appears with a much smaller splitting of about 2 meV. Furthermore, the higher lying feature has a considerably larger oscillator strength than the lower energy feature. The number of features in the  $d$  shell is consistent with those predicted by calculations. We note that for all selected symmetrical quantum dots of types 1 and 2 the same principal behavior was observed in PLE. It can be also observed for asymmetric dots, but in this case, e.g., the  $p$ -shell splitting due the asymmetry and the Coulomb induced configuration mixing cannot be distinguished.

In summary, we have studied theoretically and experimentally the evolution of the excitonic absorption spectrum of a single self-assembled quantum dot with its size. It was shown that the absorption spectrum of the  $p$  shell splits into two lines when higher electronic shells in the

dot appear. The splitting was shown to be an example of the nontrivial mixing of resonant configurations in the interacting electron-hole complex. This experiment demonstrates the high degree of control and tunability of interacting electronic systems in quantum dots.

G. A. N. thanks FAPESP-Brazil for financial support. The work was supported by the State of Bavaria.

---

\*Permanent address: Instituto de Física “Gleb Wataghin”-DFESCM, Universidade Estadual de Campinas, CP 6166 Campinas 13083-970, São Paulo, Brazil.

- [1] G. W. Bryant, Phys. Rev. B **37**, 8763 (1988); Y. Z. Hu *et al.*, Phys. Rev. B **42**, 1713 (1990); V. Halonen *et al.*, Phys. Rev. B **45**, 5980 (1992); W. Que, Phys. Rev. B **45**, 11 036 (1992); U. Bockelmann, Phys. Rev. B **48**, 17 637 (1993); Selvakumar V. Nair and Toshihide Takagahara, Phys. Rev. B **55**, 5153 (1997); Alberto Franceschetti and Alex Zunger, Phys. Rev. Lett. **78**, 915 (1997).
- [2] P. Hawrylak *et al.*, Physica (Amsterdam) **2E**, 652 (1998).
- [3] L. Jacak, P. Hawrylak, and A. Wojs, *Quantum Dots* (Springer-Verlag, Berlin, 1998); T. Chakraborty, Comments Condens. Matter Phys. **16**, 35 (1992).
- [4] P. Hawrylak, S. Fafard, and Z. Wasilewski, Condens. Matter News **7**, 16 (1999).
- [5] K. Brunner *et al.*, Phys. Rev. Lett. **69**, 3216 (1992); A. Zrenner *et al.*, Phys. Rev. Lett. **72**, 3382 (1994); D. Gammon *et al.*, Science **273**, 87 (1996); **277**, 85 (1997); Phys. Rev. Lett. **76**, 3005 (1996); M. Bayer *et al.*, Phys. Rev. Lett. **82**, 1748 (1999); A. Kuther *et al.*, Phys. Rev. B **58**, 7508 (1998); L. Landin *et al.*, Science **280**, 262 (1998); E. Dekel *et al.*, Phys. Rev. Lett. **80**, 4991 (1998).
- [6] A. Zrenner *et al.*, J. Electron. Mater. **28**, 542 (1999).
- [7] R. J. Warburton *et al.*, Phys. Rev. Lett. **79**, 5282 (1997).
- [8] A. Wojs, P. Hawrylak, S. Fafard, and L. Jacak, Phys. Rev. B **54**, 5604 (1996); P. Hawrylak, Phys. Rev. B **60**, 5597 (1999).
- [9] R. Rinaldi *et al.*, Phys. Rev. Lett. **77**, 342 (1996).
- [10] S. Raymond *et al.*, Phys. Rev. B **54**, 11 548 (1996).
- [11] L. W. Wang, A. J. Williamson, A. Zunger, H. Jiang, and J. Singh, Appl. Phys. Lett. **76**, 339 (2000).